Cache-Persistence-Aware Response-Time Analysis for Fixed-Priority Preemptive Systems

Syed Aftab Rashid*, Geoffrey Nelissen*, Damien Hardy‡, Benny Akesson*, Isabelle Puaut‡, Eduardo Tovar*
* CISTER/INESC TEC, ISEP, Polytechnic Institute of Porto, Portugal
‡ University of Rennes 1/IRISA, France

***Abstract*—A task can be preempted by several jobs of higher priority tasks during its response time. Assuming the worst-case memory demand for each of these jobs leads to pessimistic worst-case response time (WCRT) estimations. Indeed, there is a big chance that a large portion of the instructions and data associated with the preempting task τ_j are still available in the cache when τ_j releases its next jobs. Accounting for this observation allows the pessimism of WCRT analysis to be significantly reduced, which is not considered by existing work.**

The four main contributions of this paper are: 1) The concept of *persistent cache blocks* is introduced in the context of WCRT analysis, which allows re-use of cache blocks to be captured, 2) A cache-persistence-aware WCRT analysis for fixed-priority preemptive systems exploiting the PCBs to reduce the WCRT bound, 3) A multi-set extension of the analysis that further improves the WCRT bound and 4) An evaluation showing that our cache-persistence-aware WCRT analysis results in up to 10% higher schedulability than state-of-the-art approaches.

I. Introduction

The existing gap between the processor and main memory operating speeds necessitates the use of intermediate cache memories to reduce the average access time to instructions and data required by the processor. The introduction of cache memories in modern computing platforms causes big variations in the execution time of each instruction, depending on whether the instruction and data it requires are already loaded in the cache (cache hit) or not (cache miss).

Recent years have focused on analyzing the impact of preemptions on the worst-case execution time (WCET) and worst-case response time (WCRT) of tasks in preemptive systems. Indeed, the preempted tasks may suffer additional cache misses if its memory blocks are evicted from the cache during the execution of preempting tasks. These evictions cause extra accesses to main memory, which result in additional delays in the task execution. This extra cost is usually referred to as cache-related preemption delays (CRPDs).

Many different approaches have been proposed to counter the effect of preemptions. Some (e.g., [1], [2]) use non-preemptive or limited-preemption scheduling schemes to eliminate or reduce the number of preemptions. Others [3]–[9] use information about the tasks' memory access patterns to bound and incorporate preemption costs into the WCRT analysis. These approaches differ in whether they consider the memory access patterns of the preempted task [4], the preempting tasks [3], [5], or both [5]–[9]. Regardless of this distinction, they all still result in pessimistic WCRT bounds due to the fact that they only consider the effect of preemptions on the memory demand of the preempted task, but not the *variation* in memory demand of the preempting tasks. Instead, they all assume that every job of a high priority task τ_j preempting a low priority task τ_i will ask for its maximum memory demand, i.e., its worst-case memory demand in isolation. Although this may be true for the first job released by the preempting task τ_j, subsequent jobs of τ_j may re-use most of the data and instructions that were already loaded in the cache during the execution of its previous jobs. Analyses that exploit this observation have been proposed for both direct-mapped [10] and set-associative caches [11]. However, these are limited to non-preemptive task sets under static scheduling and do not apply to preemptive systems with commonly used priority-based scheduling schemes.

This work addresses this issue by proposing a novel analysis that captures the re-use of cache blocks between job executions, to reduce the negative impact of preemptions on the WCRT bound. The approach presented in this work is orthogonal to state-of-the-art methods used for CRPD calculations and can be used independently with any of these methods. The four main contributions of the paper are as follows: 1) We introduce the concept of *persistent cache blocks* (PCBs) in the context of WCRT analysis. PCBs are cache blocks that, once loaded into the cache by a task τ_i will never be evicted when τ_i runs in isolation. This concept allows us to capture the re-use of cache blocks between executions of the same task and reduce the memory demand for subsequent jobs of a task, making its memory demand *variable*, 2) A cache-persistence-aware WCRT analysis for fixed-priority preemptive systems that exploits the variable memory demand of preempting tasks to reduce the WCRT bound, 3) An extension of the proposed WCRT analysis to a multi-set approach that further improves the WCRT bound by considering the total memory demand of the preempting tasks over a task response time rather than the worst-case memory demand of each independent job, and 4) An experimental evaluation showing that our cache-persistence-aware WCRT analysis results in up to 10% higher schedulability than state-of-the-art approaches.

The rest of the paper is organized as follows. Section II presents the system model, while Section III discusses the state-of-the-art in CRPD calculation. Section IV then motivates our approach and introduces the key concept of persistent cache blocks. The basic cache-persistence-aware WCRT analysis is presented in Section V and is then extended to a multi-set approach in Section VI. Section VII explains how the inputs for our approach are obtained using static analysis, before experimental results are presented in Section VIII. Lastly, conclusions are drawn in Section IX.

II. System Model

This work targets single-core platforms with a single level (L1) data/instruction cache. The cache is assumed to be direct-mapped, which means that each memory block in the main memory can be mapped to only one block in the cache.

We consider sporadic tasks with constrained deadlines where each task has a fixed priority. Any priority assignment scheme (e.g., Rate Monotonic [12]) is acceptable. We also assume that the tasks are independent and do not suspend themselves during their execution. A task τ_i is defined by a triplet (C_i, T_i, D_i), where C_i is the WCET of τ_i, T_i is its minimum inter-arrival time and D_i is the relative deadline of each instance (or job) of τ_i. We assume that the tasks have constrained deadlines, i.e., $D_i \leq T_i$. Similarly to [13], we further decompose each task WCET into separate terms for processing demand and memory demand, respectively. Here, we use two terms, namely, the worst-case processing demand P_i and the worst-case memory demand MD_i. P_i denotes the worse-case execution time of τ_i considering that every memory access is a cache hit. Consequently, it only accounts for execution requirements of the task and does not include the time needed to fetch data and instructions from the main memory. MD_i is the worst-case memory demand of any job of task τ_i, that is, it is the maximum time during which any job of τ_i is performing memory operations. The values for C_i, P_i and MD_i are calculated assuming τ_i executes in isolation. It is also important to note that the worst-case processing demand and the worst-case memory demand may not necessarily be experienced on the same execution path of τ_i, as a result it holds that $C_i \leq P_i + MD_i$.

The WCRT of task τ_i is denoted by R_i and is defined as the longest time between the arrival and the completion of any of its jobs. A task τ_i is said to be schedulable if $R_i \leq D_i$. Similarly, a task set is schedulable if all of its tasks are schedulable.

In this work, we consider that preemption costs only refer to additional cache reloads due to those preemptions. Other overheads, e.g. due to context switches, scheduler invocations and pipeline flushes are assumed to be included in the WCET. The worst-case reload time of a cache block is denoted by d_{mem}.

We define the following task sets:

- $\mathrm{hp}(i)$: the set of tasks with higher priority than τ_i.
- $\mathrm{hep}(i)$: the set of tasks with priorities higher than or equal to τ_i.
- $\mathrm{aff}(i,j)$: the set of tasks with priorities higher than or equal to the priority of τ_i (including τ_i), but strictly lower than that of τ_j. This set contains the intermediate priority tasks, which may affect the response time of τ_i, but may also be preempted by τ_j.

III. Background

This section discusses state-of-the-art methods in more detail and establish the formal framework on which we later build our analysis. As previously mentioned, when a task τ_i is preempted by a higher priority task τ_j, it is likely that τ_j will evict memory blocks of τ_i from the cache. On resumption, τ_i might consequently have to reload cache blocks from the main memory along with its normal memory requirements. This CRPD caused by τ_j on τ_i is denoted by $\gamma_{i,j}$. Several methods have been proposed in the literature to compute $\gamma_{i,j}$. In one of the earlier works, Lee et al. [4] introduced the concept of *useful cache block* (UCB), and defined it as , *"a memory block m is called a useful cache block (UCB) at program point P, if it is cached at P and will be reused at program point Q that may be reached from P without eviction of m"*. This definition was later improved by Altmeyer et al. [14], however in this work we only use the basic concept provided in [4]. Lee et al. [4] used the maximum number of UCBs among all the tasks in $\mathrm{aff}(i,j)$ to upper bound the preemption cost $\gamma_{i,j}$. Busquets et al. [3] and Tomiyama et al. [5] rather used the notion of *evicting cache block* (ECB), i.e, any cache block accessed during the execution of the task and which can then evict the memory block cached by another task, to upper bound the preemption cost that can be caused by each preempting task. Other approaches by Tan and Mooney [7], Staschulat et al. [6] and Altmeyer et al. [8] used both the UCBs of the preempted tasks and ECBs of the preempting tasks in order to come up with more precise bounds on the preemption cost. Notably, the ECB and UCB-union and the multi-set approaches presented in [8] and [9] dominate all the existing approaches for CRPD calculation. We first detail the ECB-union approach and then the UCB-union multi-set. The formulations for the UCB-union and ECB-union multi-set can be found in [9].

The ECB-union approach [8] uses the ECBs of all tasks in $\mathrm{hep}(j)$ maximized over the UCBs of tasks in $\mathrm{aff}(i,j)$ to calculate the preemption cost $\gamma_{i,j}$. The resulting value for the preemption cost, denoted as $\gamma^{ecb}_{i,j}$, is given by

$$\gamma^{ecb}_{i,j} = d_{mem} \times \max_{\forall k \in \mathrm{aff}(i,j)} \left(\left| UCB_k \cap \left(\bigcup_{\forall l \in \mathrm{hep}(j)} ECB_l \right) \right| \right) \quad (1)$$

where d_{mem} is the time required to reload one memory block from the main memory to the cache, and UCB_k and ECB_j are the sets of UCBs and ECBs of task τ_k and τ_j, respectively. The preemption cost can then be accounted for in the WCRT analysis using the following formulation:

$$R^{ecb}_i = C_i + \sum_{\forall j \in \mathrm{hp}(i)} \left\lceil \frac{R^{ecb}_i}{T_j} \right\rceil \times (C_j + \gamma^{ecb}_{i,j}) \quad (2)$$

When combined, the ECB and UCB-union approaches provide a reasonably precise upper bound on the preemption cost. However, it can also lead to over-estimations in different situations, as shown in [9]. This is due to the fact that both ECB and UCB-union approaches do not take into account the actual number of preemptions of each low and intermediate priority task. For instance, with these approaches it is assumed that a high priority task τ_j can preempt any task $\tau_k \in \mathrm{aff}(i,j)$ the same number of times it can preempt τ_i. This can only be true if $\tau_k = \tau_i$, and will lead to over-estimation in all other cases where the cost of τ_j preempting τ_k is higher than the preemption cost of τ_j on τ_i.

To reduce this pessimism associated to the ECB and UCB-union approaches, Altmeyer et al. [9] proposed two new solutions, namely, the UCB-union multi-set and the ECB-union

multi-set approaches. These multi-set versions of the UCB-union and ECB-union approaches additionally take into account the maximum number of jobs $E_j(R_i) \stackrel{\text{def}}{=} \left\lceil \frac{R_i}{T_j} \right\rceil$ that each higher priority task τ_j can release during the response time of τ_i and the number of preemptions of each low and intermediate priority task by τ_j, i.e., $E_j(R_k)E_k(R_i) \stackrel{\text{def}}{=} \left\lceil \frac{R_k}{T_j} \right\rceil \times \left\lceil \frac{R_i}{T_k} \right\rceil$. Under this framework, the WCRT equation becomes:

$$R_i^{mul} = C_i + \sum_{\forall j \in \text{hp}(i)} \left\lceil \frac{R_i^{mul}}{T_j} \right\rceil \times C_j + \sum_{\forall j \in \text{hp}(i)} \gamma_{i,j}^{mul} \quad (3)$$

where $\gamma_{i,j}^{mul}$ accounts for the total preemption cost that can be caused by all jobs of τ_j released during the response time of τ_i. We detail the UCB-union multi-set approach and refer the reader to [9] for the ECB-union multi-set formulation. Using the UCB-union multi-set approach $\gamma_{i,j}^{mul}$ is upper bounded by $\gamma_{i,j}^{ucb-m}$ defined as follows:

$$\gamma_{i,j}^{ucb-m} = d_{mem} \times \left| M_{i,j}^{ucb} \cap M_{i,j}^{ecb} \right| \quad (4)$$

where $M_{i,j}^{ucb}$ and $M_{i,j}^{ecb}$ are multi-sets defined as

$$M_{i,j}^{ucb} = \bigcup_{\forall k \in \text{aff}(i,j)} \left(\bigcup_{E_j(R_k)E_k(R_i)} UCB_k \right) \quad (5)$$

and

$$M_{i,j}^{ecb} = \bigcup_{E_j(R_i)} ECB_j \quad (6)$$

Here, $M_{i,j}^{ucb}$ is a multi-set comprising sets of UCBs of all low and intermediate priority tasks $\in$ aff(i,j) added $E_j(R_k)E_k(R_i)$ times, i.e., the maximum number of times τ_j can preempt each τ_k during the response time of τ_i. Similarly, $M_{i,j}^{ecb}$ is a multi-set comprising the set of ECBs of all jobs of τ_j executing within the response time of τ_i. The final value of the preemption cost $\gamma_{i,j}^{ucb-m}$ comes from the intersection of both these multi-sets.

The construction of the ECB-union multi-set approach is analogous to the UCB-union multi-set approach. Note that the ECB-union multi-set approach dominates the ECB-union approach [8], while the UCB-union multi-set approach dominates the UCB-union approach [7]. Yet, it is shown in [9] that the ECB-union and UCB-union multi-set approaches are incomparable. For a more detailed description of the formulation of Equations (2) to (6), the reader is referred to [9].

IV. Problem Definition

In this section, first we provide a basic example to affirm the motivation behind this work. Later, using this example as a base we provide some useful definitions that will be used in rest of the paper.

A. Motivational Example

As presented in the previous section, the impact of a high priority task τ_j on the WCRT of any lower priority task τ_i can be estimated in a fairly accurate manner by analyzing the mapping of UCBs and ECBs in the cache. However, the impact of τ_i on the memory demand of τ_j is ignored during the WCRT analysis of τ_i. Yet, high priority tasks may often execute more than one job during the response time of a lower priority task. Therefore, to accurately estimate the WCRT of a low priority task τ_i, one must consider the impact of the preempted tasks on the memory demand of each job released by the preempting tasks. In the literature, this is dealt with by assuming that the memory demand for each job of a high priority task τ_j executing within the response time of a low priority task τ_i is always maximum, i.e, equal to the maximum memory demand MD_j. Following that assumption, the total memory overhead MO_i that must be accounted by τ_i during its worst-case response time is upper bounded by the following equation derived in [15].

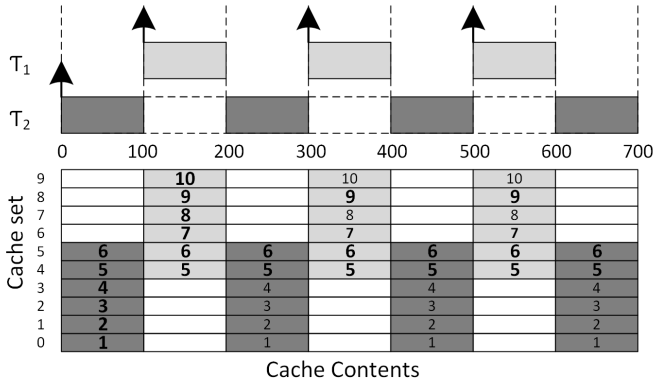

Fig. 1: Schedule and cache contents for a taskset $\{\tau_1, \tau_2\}$ with $C_1 = 100$, $C_2 = 400$, $MD_1 = 60$, $MD_2 = 80$, $ECB_1 = \{5,6,7,8,9,10\}$, $ECB_2 = \{1,2,3,4,5,6\}$, $UCB_1 = \{6,7\}$, $UCB_2 = \{5,6\}$, $PCB_1 = \{5,6,7,8,10\}$ and $PCB_2 = \{1,2\}$. The schedule assumes that τ_1 releases its first job with an offset of 100 time units.

$$MO_i = MD_i + \sum_{\forall j \in hp(i)} \left\lceil \frac{R_i}{T_j} \right\rceil \times (MD_j + \gamma_{i,j}) \quad (7)$$

There is a significant level of pessimism involved in Equation (7), as we will demonstrate using the example below.

Example 1. *Consider the two tasks τ_1 and τ_2 (where τ_1 has a higher priority than τ_2) presented in Figure 1. We assume that the time d_{mem} needed to access the main memory and load a memory block to the cache is equal to 10 time units and that the memory demand of τ_1 and τ_2 are $MD_1 = 60$ and $MD_2 = 80$[1], respectively. We also assume that memory block $\{9\}$ accessed by τ_1 contains data that must be updated at the beginning of the execution of each of its jobs. Figure 1 depicts a possible schedule together with the evolution of the cache contents over time. The memory blocks that must be loaded/reloaded from the main memory after each preemption or resumption are shown in bold with a bigger font size in Figure 1.*

Initially, the cache is empty and τ_2 loads all its ECBs from the main memory as soon as it starts to execute. When τ_1 preempts τ_2 for the first time, it also loads all its ECBs into the

[1]Note that because the same cache block may be used by several memory blocks of the same task τ_i, the worst-case memory demand MD_i of τ_i may be larger than the number of ECBs of τ_i multiplied by d_{mem}.

cache with a memory demand of $MD_1 = 60$. Since there is an overlap between the mapping of ECBs of τ_1 and the mapping of UCBs of τ_2 in the cache, τ_1 evicts some of the useful cache blocks of τ_2. In turn, when τ_2 resumes its execution, it has to account for $\gamma_{2,1} = 2 \times d_{mem} = 20$, in order to load cache blocks $\{5, 6\}$ again from main memory. However, when the second job of τ_1 preempts τ_2, one can notice that it no longer needs to reload all of its ECBs. In fact, most of the memory blocks needed by τ_1 are still in the cache. As a consequence, τ_1 must only reload memory blocks $\{5, 6\}$, which have been evicted by τ_2, as well as memory block $\{9\}$ that must be reloaded for each new job execution of τ_1. The same scenario happens for all jobs released by τ_1, except the first one. The actual memory demand for the second and third job of τ_1 is hence much less (i.e., 30) than $MD_1 = 60$, illustrating that it is not constant across all job executions.

In the presented example, memory blocks $\{5, 6, 7, 8, 10\}$ are called *persistent cache blocks* (PCBs), as they are never evicted from the cache once loaded when τ_1 executes in isolation. In contrast, cache block $\{9\}$ is a *non-persistent cache block* (nPCB). nPCBs may be cache blocks that are shared by several memory blocks of the same task, or simply data (e.g., sensor readings, value on an input port, global shared data) that must be reloaded before each access. One must note that PCBs and nPCBs are different from the notions of UCBs and ECBs in the sense that it does not matter if they are referenced more than once during a single execution of a task. However, a PCB must never be evicted from the cache by the task itself once it is fetched from main memory.

The state-of-the-art does not consider PCBs while calculating the memory overhead suffered by a task τ_i in case of preemptions. This results in pessimistic memory overhead evaluations and hence pessimistic WCRT computations. This can easily be shown using the example in Figure 1. If τ_2's memory overhead is computed using Equation (7), one would get:

$$MO_2 = MD_2 + 3 \times MD_1 + 3 \times \gamma_{2,1} = 80 + 3 \times 60 + 3 \times 20 = 320$$

Equation (7) considers the worst-case memory demand, i.e., MD_1 for each job of τ_1 that executes during the response time of τ_2. As we have shown in Example 1, the actual memory demand of the second and third job of τ_1 is in fact much less. Considering the PCBs of τ_1 while calculating the memory overhead MO_2, the resulting value is given as:

$$\begin{aligned} MO_2 &= MD_2 + MD_1 + 2 \times (MD_1 - |PCB_1| \times d_{mem}) \\ &\quad + 3 \times \gamma_{2,1} \\ &= 80 + 60 + 2 \times (60 - 5 \times 10) + 3 \times 20 = 220 \end{aligned}$$

This simple example highlights the necessity to consider PCBs when calculating the memory demand and hence the WCRT of a task.

B. Problem Formalization

The previous example casually introduced the notions of PCB and nPCB. We now formally define those two types of cache blocks associated to the execution of a task τ_i.

Definition 1 (Persistent cache block)**.** A memory block of a task τ_i is persistent if once loaded by τ_i, it will never be invalidated or evicted from the cache when τ_i executes in isolation.

Definition 2 (Non-persistent cache block)**.** A non-persistent cache block (nPCB) of task τ_i is an ECB that is not a PCB. That is, it is a memory block that may need to be reloaded at some point during the execution of τ_i (in the same or different jobs), even when τ_i executes in isolation.

The sets of PCBs and nPCBs associated to a task τ_i are denoted by PCB_i and $nPCB_i$, respectively. It follows from the two previous definitions that each cache block associated to a task τ_i (ECB_i) is either a PCB or a nPCB, hence the following two relations:

$$PCB_i \cup nPCB_i = ECB_i \tag{8}$$

$$PCB_i \cap nPCB_i = \emptyset \tag{9}$$

By Definition 1, if τ_i executes in isolation, a PCB is loaded only once from the main memory and hence contributes only once to the total memory demand of τ_i. Even though all the ECBs of τ_i (i.e., PCBs and nPCBs) contribute to its worst-case memory demand in isolation (i.e., MD_i), only the nPCBs, a subset of ECB_i, must be loaded by more than one job of τ_i. Considering the worst-case memory demand for each job released by higher priority tasks than τ_i when computing the WCRT of τ_i, as is implicitly the case in Equations (2) and (3), is thus pessimistic. Therefore, we define the *residual memory demand* of a task τ_i as the worst-case memory demand of τ_i assuming that all the PCBs of τ_i are already in the cache memory and therefore result in cache hits when being accessed.

Definition 3 (Residual memory demand)**.** The residual memory demand MD_i^r of task τ_i is the worst-case memory demand over all the jobs of τ_i when all its PCBs are already loaded in the cache memory. Therefore, MD_i^r only accounts for the accesses to the nPCBs of τ_i and can occur during any job execution of τ_i.

An upper bound on the total memory demand $MD_i(t)$ of a task τ_i within a time window of length t when τ_i executes in isolation is proven in the following lemma.

Lemma 1. If a task τ_i executes in isolation, then its total memory demand $MD_i(t)$ within a time window of length t is upper bounded by $\hat{MD}_i(t)$ where

$$\begin{aligned} \hat{MD}_i(t) \stackrel{\text{def}}{=} \min \Bigg\{ & \left\lceil \frac{t}{T_i} \right\rceil MD_i \ ; \\ & \left\lceil \frac{t}{T_i} \right\rceil MD_i^r + \mid PCB_i \mid \times d_{mem} \Bigg\} \end{aligned} \tag{10}$$

Proof. We prove that $\left\lceil \frac{t}{T_i} \right\rceil MD_i$ and $\left\lceil \frac{t}{T_i} \right\rceil MD_i^r + \mid PCB_i \mid \times d_{mem}$ are both upper bounds on the total memory demand $MD_i(t)$ of τ_i. Thus, the minimum of those bounds is also an upper bound on $MD_i(t)$.

1) τ_i can release at most $\left\lceil \frac{t}{T_i} \right\rceil$ jobs in a time window of length t. By definition of MD_i, each of these jobs has a worst-case memory demand MD_i. Therefore, $\left\lceil \frac{t}{T_i} \right\rceil MD_i$ is an upper bound on the total memory demand of τ_i.
2) Recall from Equations (8) and (9) that $PCB_i \cup nPCB_i = ECB_i$ and $PCB_i \cap nPCB_i = \emptyset$. Characterizing the worst-case contribution of the PCBs and nPCBs to the total

memory demand is therefore sufficient to quantify the worst-case contribution of all the cache blocks of τ_i to $MD_i(t)$. Since by Definition 1, the persistent cache blocks must be loaded only once, the maximum contribution of the cache blocks in PCB_i to $MD_i(t)$ is $\mid PCB_i \mid \times d_{mem}$ (i.e., the total number of PCBs times the worst-case memory access time). By Definition 3, the worst-case contribution of nPCBs to the memory demand of each job released by τ_i is MD_i^r. Since a maximum of $\left\lceil \frac{t}{T_i} \right\rceil$ jobs are released by τ_i in a time window of length t, an upper bound on the total contribution of the nPCBs to $MD_i(t)$ is given by $\left\lceil \frac{t}{T_i} \right\rceil MD_i^r$. Adding the contributions of nPCBs and PCBs, we get that $\left\lceil \frac{t}{T_i} \right\rceil MD_i^r + \mid PCB_i \mid \times d_{mem}$ is an upper bound on the total memory demand of τ_i.

□

Although Equation (10) provides an upper bound on the total memory demand of τ_i in *isolation*, the total memory demand of τ_i when executing concurrently with other tasks can be much larger. Indeed, as can be observed in Example 1, the PCBs of a task τ_j can be evicted due to the execution of any task (i.e. tasks in $\mathrm{hep}(i) \setminus \tau_j$) between the execution of two successive jobs of τ_j. This requires the effect of all tasks in $\mathrm{hep}(i) \setminus \tau_j$ on the memory demand of $\tau_j \in \mathrm{hp}(i)$ during the WCRT of τ_i to be taken into account. We refer to this extra memory demand caused by the eviction of PCBs of τ_j by the tasks in $\mathrm{hep}(i) \setminus \tau_j$ as *cache-persistence reload overhead* (CPRO) and denote it by $\rho_{j,i}$. CPRO is formally defined as:

Definition 4 (Cache-persistence reload overhead)**.** Cache-persistence reload overhead, denoted by $\rho_{j,i}$, is the maximum memory overhead of any task τ_j due to eviction of its PCBs resulting from the execution of all tasks in $\mathrm{hep}(i) \setminus \tau_j$, while τ_j is executing during the response time of τ_i.

V. CPRO-union Approach

In this section, we present a simple approach similar to the ECB-union to calculate the CPRO (i.e. $\rho_{j,i}$). We further demonstrate how $\rho_{j,i}$ can be incorporated in the WCRT analysis of a task τ_i. Later, in Section VI, we extend this simple union approach into a multi-set variant to remove some of the pessimism associated with this analysis.

A. Computation of Cache-Persistence Reload Overhead

As discussed in Section IV-B, $\rho_{j,i}$ accounts for the extra memory demand of each job of $\tau_j \in \mathrm{hp}(i)$ due to evictions of its persistent cache blocks by other tasks running concurrently on the processor.

As one can see in Figure 1, the PCBs of a task $\tau_j \in \mathrm{hp}(i)$ can be evicted by the ECBs of any other task running on the platform between two successive jobs of τ_j. The memory demand overhead $\rho_{i,j}$ can thus be upper bounded by the intersection of the set PCB_j of all PCBs of τ_j with all cache blocks (i.e., ECBs) that can be loaded by any other task between two executions of τ_j. This observation leads to the following theorem.

Theorem 1. The cache-persistence reload overhead imposed by the eviction of PCBs of a job of task $\tau_j \in \mathrm{hp}(i)$ on the worst-case response time of a task τ_i is upper bounded by

$$\rho_{j,i} = d_{mem} \times \left| PCB_j \cap \Big(\bigcup_{\forall \tau_k \in \mathrm{hep}(i) \setminus \tau_j} ECB_k \Big) \right| \tag{11}$$

Proof. Since a fixed-priority scheduling algorithm is used, only tasks with priorities higher than or equal to the priority of τ_i (i.e., tasks in $\mathrm{hep}(i)$) can execute during the response time of τ_i. Therefore, any task $\tau_k \in \mathrm{hep}(i) \setminus \tau_j$ can execute between two subsequent jobs of τ_j and hence evict some or all the PCBs of τ_j.

The worst-case memory interference of any task $\tau_k \in \mathrm{hep}(i) \setminus \tau_j$ on τ_j is when it reloads all its cache blocks (i.e., its ECBs) between two subsequent jobs of τ_j. Therefore, the largest set of memory blocks loaded by tasks in $\mathrm{hep}(i) \setminus \tau_j$ between two jobs of τ_j is given by $\bigcup_{\forall \tau_k \in \mathrm{hep}(i) \setminus \tau_j} ECB_k$.

The set of persistent cache blocks that must be reloaded by τ_j during each job execution is thus upper bounded by the intersection between τ_j's PCBs (i.e., PCB_j) and $\bigcup_{\forall \tau_k \in \mathrm{hep}(i) \setminus \tau_j} ECB_k$.

Since each cache block reload takes at most d_{mem} time units, the CPRO due to the eviction of PCBs of τ_j by tasks in $\mathrm{hep}(i) \setminus \tau_j$ is upper bounded by

$$d_{mem} \times \left| PCB_j \cap \Big(\bigcup_{\forall \tau_k \in \mathrm{hep}(i) \setminus \tau_j} ECB_k \Big) \right|$$

□

Having defined an expression to calculate $\rho_{j,i}$, we now define $\rho_{j,i}(t)$, i.e., the total cache-persistence reload overhead on τ_j in a time window of length t due to the eviction of its PCBs by tasks in $\mathrm{hep}(i) \setminus \tau_j$. $\rho_{j,i}(t)$ tells us by how much the memory demand of τ_j can vary in comparison to its memory demand in isolation (i.e., $MD_j(t)$) due to the interference generated by the other tasks executing concurrently with τ_j. Using Theorem 1, $\rho_{j,i}(t)$ can be easily computed as stated in Lemma 2 below.

Lemma 2. The total CPRO $\rho_{j,i}(t)$ on the execution time of τ_j due to the eviction of its PCBs by tasks in $\mathrm{hep}(i) \setminus \tau_j$ in a time interval of length t is upper bounded by $\hat{\rho}_{j,i}(t)$ where

$$\hat{\rho}_{j,i}(t) \stackrel{\text{def}}{=} \left(\left\lceil \frac{t}{T_j} \right\rceil - 1 \right) \times \rho_{j,i} \tag{12}$$

Proof. It directly follows from the fact that τ_j releases at most $\left\lceil \frac{t}{T_j} \right\rceil$ jobs in a time interval of length t. As a result, at most $\left(\left\lceil \frac{t}{T_j} \right\rceil - 1 \right)$ evictions can happen *between* two subsequent jobs of τ_j. Since by Theorem 1, the CPRO suffered by a job of τ_j is upper bounded by $\rho_{j,i}$, the total overhead $\rho_{j,i}(t)$ is upper bounded by $\left(\left\lceil \frac{t}{T_j} \right\rceil - 1 \right) \times \rho_{j,i}$. □

B. WCRT Analysis

After showing how the extra memory demand overhead $\rho_{j,i}$ of a high priority task τ_j can be computed, we now

describe how it can be integrated into the WCRT analysis of any lower priority task τ_i. As mentioned in Section III, the WCRT analysis for fixed-priority preemptive systems was first presented in [16], [17] without considering memory overheads due to preemptions. It was then extended in several works (e.g., [3], [8], [9]) to account for the cache-related preemption delays. Some of the most prominent approaches resulted in Equations (2) and (3), previously presented in Section III.

Although these approaches are beneficial, their WCRT analysis still rely exclusively on the WCET C_j of high priority tasks when computing the worst-case response time of a low priority task τ_i. That is, it assumes that each job of a task $\tau_j \in \mathrm{hp}(i)$ executing within the response time of τ_i asks for its worst-case memory demand MD_j. As discussed in Section IV, this assumption is pessimistic. In fact, due to the existence of persistent cache blocks, once τ_j loads all its ECBs (i.e., PCBs and nPCBs), subsequent jobs of τ_j will only need to reload nPCBs and some of the PCBs that may have been evicted due to the execution of tasks in $\mathrm{hep}(i) \setminus \tau_j$. As a result, for subsequent jobs of τ_j the memory demand will be significantly lower than MD_j. To exploit this variable memory demand, we present a more elaborate formulation of the WCRT analysis. We propose that for any task τ_i the WCRT of task τ_i is upper bounded by the smallest positive value R_i such that

$$R_i = C_i + \sum_{\forall j \in \mathrm{hp}(i)} (P_j(R_i) + MD_j(R_i) + \rho_{j,i}(R_i) + \gamma_{i,j}(R_i)) \quad (13)$$

In this WCRT formulation, we separately account for the maximum processing demand $P_j(R_i)$ and memory demand $MD_j(R_i)$ (in isolation) that can be claimed by each higher priority task τ_j within the response time R_i of τ_i. The terms $\rho_{j,i}(R_i)$ and $\gamma_{i,j}(R_i)$ denote the total cache-persistence reload overhead due to the eviction of PCBs of τ_j by tasks in $\mathrm{hep}(i) \setminus \tau_j$, and the total cache-related preemption delay due to the preemptions caused by τ_j within the response time of τ_i, respectively. The terms $(P_j(R_i) + MD_j(R_i))$ assume values obtained in isolation, while the two last terms $(\rho_{j,i}(R_i) + \gamma_{i,j}(R_i))$ account for the overheads introduced by the eviction of cache blocks by other tasks sharing the cache.

As already discussed in Section III, $\gamma_{i,j}(R_i)$ is upper bounded by $\gamma^{mul}_{i,j}$. Furthermore, as proven in Lemmas 1 and 2, $MD_j(R_i)$ and $\rho_{j,i}(R_i)$ are upper bounded by Equations (10) and (12), respectively. Finally, because each task τ_j releases at most $\left\lceil \frac{t}{T_j} \right\rceil$ jobs in a time window of length t, $P_j(R_i)$ is smaller than or equal to $\left\lceil \frac{R_i}{T_j} \right\rceil P_j$.

Replacing each term with its given bound, we get that

$$R_i \leq C_i + \sum_{\forall j \in \mathrm{hp}(i)} \left\lceil \frac{R_i}{T_j} \right\rceil P_j + \sum_{\forall j \in \mathrm{hp}(i)} \hat{MD}_j(R_i) + \sum_{\forall j \in \mathrm{hp}(i)} \hat{\rho}_{j,i}(R_i) + \sum_{\forall j \in \mathrm{hp}(i)} \gamma^{mul}_{i,j} \quad (14)$$

In systems where the number of PCBs is high and the cache interference is low, the value provided by $\hat{MD}_j(R_i) + \hat{\rho}_{j,i}(R_i)$ should always be smaller than $\left\lceil \frac{R_i}{T_j} \right\rceil MD_i$, and therefore we should often have $\left\lceil \frac{R_i}{T_j} \right\rceil P_j + \hat{MD}_j(t) + \hat{\rho}_{j,i}(R_i)$ smaller than $\left\lceil \frac{R_i}{T_j} \right\rceil C_j$. In this case, Equation (14) will result in a tighter WCRT bound than Equation (3). However, in some situations, since $\hat{MD}_j(t)$ and $\hat{\rho}_{j,i}(R_i)$ are upper bounds and not exact values, this formulation can result in an over-estimation of the interference generated by τ_j on τ_i. In order to counter this effect, and knowing that Equation (3) is already an upper bound on the WCRT of τ_i, we further improve Equation (14) by always taking the minimum between $\left\lceil \frac{R_i}{T_j} \right\rceil C_j$ and $\left\lceil \frac{R_i}{T_j} \right\rceil P_j + \hat{MD}_j(t) + \hat{\rho}_{j,i}(R_i)$ as the total interference caused by τ_j on τ_i (see Equation (15) below). Following this simple modification to Equation (14), Equation (15) will always return a value that is smaller than or equal to the solution to Equation (3). Our approach hence dominates the UCB union multi-set approach defined in [9].

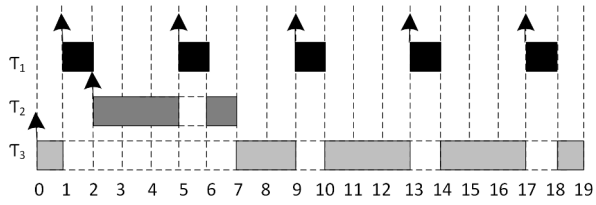

Fig. 2: Illustration of the pessimism associated with Equation (12) using the task set $\{\tau_1, \tau_2\, \tau_3\}$ when τ_1 and τ_2 releasing their first jobs with an offset.

$$R^{un}_i = C_i + \sum_{\forall j \in \mathrm{hp}(i)} \min \left\{ \left\lceil \frac{R^{un}_i}{T_j} \right\rceil C_j \; ; \left\lceil \frac{R^{un}_i}{T_j} \right\rceil P_j + \hat{MD}_j(R^{un}_i) + \hat{\rho}_{j,i}(R^{un}_i) \right\} + \sum_{\forall j \in \mathrm{hp}(i)} \gamma^{mul}_{i,j} \quad (15)$$

Note that Equation (15) is recursive. However, a solution can be found using simple fixed-point iteration on R^{un}_i initiating R^{un}_i to C_i. The iteration stops as soon as R^{un}_i does not evolve anymore or $R^{un}_i > D_i$, in which case the task is deemed unschedulable.

VI. CPRO Multi-Set Approach

The formulation in Equations (11) and (12) considers the ECBs of all tasks $\tau_k \in \mathrm{hep}(i) \setminus \tau_j$ as interfering with every job of τ_j released within the response time of τ_i. This is pessimistic. Indeed, considering two different tasks τ_k and τ_l pertaining to $\mathrm{hep}(i) \setminus \tau_j$, the number of times τ_l can execute between two successive jobs of τ_j is not necessarily equal to the number of times τ_k can execute between two successive jobs of τ_j. This situation is discussed in Example 2.

Example 2. *Let* $\tau_1 = (1, 4, 4)$, $\tau_2 = (4, 30, 30)$ *and* $\tau_3 = (10, 50, 50)$, *where* τ_1 *has the highest priority and* τ_3 *the lowest. Figure 2 presents a possible schedule that generates the worst-case response time of* τ_3. *As one can see,* τ_1 *releases* 5 *jobs during the response time of* τ_3. *As a result, Equation* (15) *upper bounds the total cache overheads on the PCBs of* τ_1 *with* 4 *times* $\rho_{1,3}$. *That is, it assumes that both*

τ_2 and τ_3 execute and reload all their ECBs between every two successive jobs of τ_1. As can be seen in Figure 2, this is pessimistic. In fact, τ_2 execute only twice between jobs of τ_1! Its impact on the total CPRO of τ_1 is therefore clearly overestimated.

In order to reduce the pessimism associated with the computation of $\rho_{j,i}$, we must consider the actual number of times each task $\tau_k \in \text{hep}(i) \setminus \tau_j$ can execute between two successive jobs of τ_j. For this reason, this section presents a multi-set variant of Equation (12). The resulting quantity is an upper bound on $\hat{\rho}_{j,i}(t)$ denoted by $\rho^{mul}_{j,i}(t)$.

A. Computation of $\rho^{mul}_{j,i}(t)$

In this section, we first characterize the maximum number of times a task $\tau_k \in \text{hep}(i) \setminus \tau_j$ can execute between two successive jobs of τ_j. To do so, we separately analyze the tasks in $\text{hep}(j) \setminus \tau_j$ (Lemma 3) and $\text{aff}(i,j)$ (Lemma 4). We then use this information to upper bound the total cache-persistence reload overhead $\rho_{j,i}(t)$ in Theorem 2.

Lemma 3. The maximum number of times a task $\tau_k \in \text{hep}(j) \setminus \tau_j$ can execute between two successive jobs of τ_j within the response time R_i of τ_i is upper bounded by $E_k(R_i)$.

Proof. Remember that the maximum number of jobs that each higher priority task τ_k can release during the response time of a task τ_i is given by $E_k(R_i) \stackrel{\text{def}}{=} \left\lceil \frac{R_i}{T_k} \right\rceil$. Furthermore, because τ_k has a higher or equal priority than τ_j, τ_j cannot preempt τ_k. Hence, the maximum number of time τ_k can execute between two successive jobs of τ_j within a time window of length R_i is upper bounded by its number of released jobs $E_k(R_i)$ (see Figure 3 for an example). □

Lemma 4. The maximum number of times a task $\tau_k \in \text{aff}(i,j)$ can execute between two successive jobs of τ_j within the response time R_i of τ_i is upper bounded by

$$(E_j(R_k)+1) \times E_k(R_i) \tag{16}$$

Proof. $E_j(R_k) \stackrel{\text{def}}{=} \left\lceil \frac{R_k}{T_j} \right\rceil$ provides the maximum number of jobs that τ_j can release during the response time of a task τ_k. Each of these released jobs may preempt the execution of τ_k. Considering an arrival pattern such that τ_k started to execute just before the first arrival of τ_j preempting τ_k (see Figure 3), the maximum number of times a job of τ_k may execute between two successive jobs of τ_j is then given by $(E_j(R_k)+1)$. Since $E_k(R_i)$ jobs of τ_k are released within the response time of τ_i, the maximum number of times τ_k may execute between two successive jobs of τ_j within the response time of τ_i is upper bounded by $(E_j(R_k)+1) \times E_k(R_i)$. □

Using Lemmas 3 and 4, one can derive an upper bound on $\rho_{j,i}(t)$. This upper bound is denoted by $\rho^{mul}_{j,i}(t)$ and is defined in the following theorem.

Theorem 2. The total cache-persistence reload overhead $\rho_{j,i}(R_i)$ on τ_j due to the eviction of its PCBs by tasks in $\text{hep}(i) \setminus \tau_j$ during the response time R_i of τ_i is upper bounded by

$$\rho^{mul}_{j,i} \stackrel{\text{def}}{=} d_{mem} \times \left| M^{ecb}_{j,i} \cap M^{pcb}_{j,i} \right| \tag{17}$$

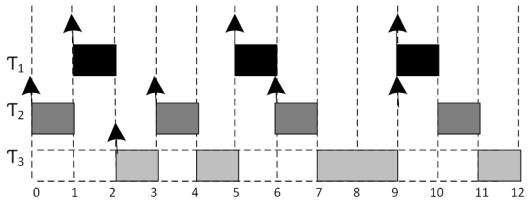

Fig. 3: Illustration of the maximum number of times the tasks in $\text{aff}(i,j)$ and $\text{hep}(j) \setminus \tau_j$ can execute between two successive jobs of τ_j. When calculating $\rho_{2,3}$, $\tau_1 \in \text{hep}(2) \setminus \tau_2$ can release maximally 3 jobs (with each job loading all its ECBs in the worst case). In contrast, the one job released by $\tau_3 \in \text{aff}(3,2)$ can execute and load its ECBs maximum 4 times.

where $M^{ecb}_{j,i}$ and $M^{pcb}_{j,i}$ are multi-sets defined as

$$M^{pcb}_{j,i} = \bigcup_{E_j(R_i)-1} PCB_j \tag{18}$$

and

$$M^{ecb}_{j,i} = M^{ecb-aff}_{j,i} \cup M^{ecb-hp}_{j,i} \tag{19}$$

with

$$M^{ecb-aff}_{j,i} = \bigcup_{\forall k \in \text{aff}(i,j)} \left(\bigcup_{(E_j(R_k)+1)E_k(R_i)} ECB_k \right) \tag{20}$$

and

$$M^{ecb-hp}_{j,i} = \bigcup_{\forall l \in \text{hep}(j) \setminus \tau_j} \left(\bigcup_{E_l(R_i)} ECB_l \right) \tag{21}$$

Proof. The proof is based on the three following facts:

1. τ_j releases at most $\left\lceil \frac{t}{T_j} \right\rceil$ jobs in a time window of length t. At most $\left(\left\lceil \frac{t}{T_j} \right\rceil - 1 \right)$ evictions can therefore happen *between* two subsequent jobs of τ_j. The largest set of PCBs of τ_j that can be evicted between successive jobs of τ_j released during the response time of τ_i is therefore given by the multi-set $M^{pcb}_{j,i} = \bigcup_{E_j(R_i)-1} PCB_j$.

2. By Lemma 3, the maximum number of times a task $\tau_l \in \text{hep}(j) \setminus \tau_j$ can execute between two successive jobs of τ_j during the response time of τ_i is upper bounded by $E_l(R_i)$. Hence, the largest set of ECBs that can be loaded by τ_l and interfere with the PCBs of τ_j is given by $\bigcup_{E_l(R_i)} ECB_l$ (assuming that τ_l reloads all its ECBs at each of its execution). This results in that the largest set of ECBs loaded by the tasks in $\text{hep}(j) \setminus \tau_j$ between successive executions of τ_j is upper bounded by $M^{ecb-hp}_{j,i} = \bigcup_{\forall l \in \text{hep}(j) \setminus \tau_j} \left(\bigcup_{E_l(R_i)} ECB_l \right)$.

3. By Lemma 4, the maximum number of times a task $\tau_k \in \text{aff}(i,j)$ can execute between two successive jobs of τ_j during the response time of τ_i is upper bounded by $(E_j(R_k)+1) \times E_k(R_i)$. Hence, the largest set of ECBs that can be loaded by τ_k between successive jobs of τ_j during the response time of τ_i is given by $\bigcup_{(E_j(R_k)+1)E_k(R_i)} ECB_k$ (assuming that τ_k reloads all its ECBs whenever it resumes its execution). This

results in that the largest set of ECBs loaded by the tasks in $\mathrm{aff}(i,j)$ between successive executions of τ_j is upper bounded by $M_{j,i}^{ecb-aff} = \bigcup_{\forall k \in \mathrm{aff}(i,j)} \left(\bigcup_{(E_j(R_k)+1)E_k(R_i)} ECB_k \right)$.

Therefore, by 2. and 3. the largest set of ECBs that can interfere with the PCBs of τ_j during the response time of τ_i is upper bounded by $M_{j,i}^{ecb} = M_{j,i}^{ecb-aff} \cup M_{j,i}^{ecb-hp}$.

Finally, the largest set of PCBs of τ_j that can be evicted by the tasks in $\mathrm{hep}(i) \setminus \tau_j$ within the response time of τ_i is upper bounded by the intersection of $M_{j,i}^{pcb}$ with $M_{j,i}^{ecb}$. Since reloading a cache block takes at most d_{mem} time units, the total cache-persistence reload overhead $\rho_{j,i}(R_i)$ is upper bounded by $d_{mem} \times \left| M_{j,i}^{ecb} \cap M_{j,i}^{pcb} \right|$. □

B. Improving the Accuracy of $M_{j,i}^{ecb}$

Theorem 2 provides a good upper bound on the total cache-persistence reload overhead $\rho_{j,i}(R_i)$ during the response time of τ_i. However, Equations (20) and (21) still consider that each job released by the tasks $\tau_k \in \mathrm{hep}(i) \setminus \tau_j$ reload all their ECBs (i.e., PCBs and nPCBs) whenever they resume their execution. Even though this assumption may be valid for the tasks $\tau_l \in \mathrm{hep}(j) \setminus \tau_j$, since each of their jobs contributes only once to $M_{j,i}^{ecb}$ (hence assuming that each job of τ_l accesses all its cache blocks during its execution), it is quite pessimistic for the tasks $\tau_k \in \mathrm{aff}(i,j)$. Indeed, by Lemma 4 and Equation (20), each job of a task $\tau_k \in \mathrm{aff}(i,j)$ is assumed to contribute $(E_j(R_k)+1)$ times to $M_{j,i}^{ecb}$. However, a PCB of task τ_k will be accessed at most once during each job execution unless this PCB is also a UCB (in which case it may be used at several program points of the task). The nPCBs must always be considered to be loaded several times during each job execution though. Indeed, since they are not persistent, it means that several memory blocks of τ_k are mapped to that same cache block, which can therefore be accessed more than once during each job execution.

It results from this discussion that $M_{j,i}^{ecb}$ can be more accurately modeled by the following equation:

$$M_{j,i}^{ecb} = M_{j,i}^{ecb-aff'} \cup M_{j,i}^{ecb-hp} \tag{22}$$

with

$$M_{j,i}^{ecb-aff'} = \bigcup_{\forall k \in \mathrm{aff}(i,j)} \left[\left(\bigcup_{E_k(R_i)} (PCB_k \setminus UCB_k) \right) \bigcup \left(\bigcup_{(E_j(R_k)+1)E_k(R_i)} \Big(nPCB_k \cup (PCB_k \cap UCB_k) \Big) \right) \right] \tag{23}$$

where $(PCB_k \cap UCB_k)$ is the set of PCBs of τ_k that are also UCBs, and $(nPCB_k \cup (PCB_k \cap UCB_k))$ is therefore the set of ECBs that may be loaded more than once by each job of τ_k. All the other ECBs (those that are not in $(nPCB_k \cup (PCB_k \cap UCB_k))$ and are thus in $(PCB_k \setminus UCB_k)$ are loaded at most once per job of τ_k and are therefore accounted separately in the first term of Equation (23).

C. WCRT Analysis

Using the exact same argumentation as in Section V-B, the worst-case response time of task τ_i can be upper bounded by the smallest positive value R_i^{mul} such that:

$$R_i^{mul} = C_i + \sum_{\forall j \in \mathrm{hp}(i)} \min \left\{ \left\lceil \frac{R_i^{mul}}{T_j} \right\rceil C_j \; ; \; \left\lceil \frac{R_i^{mul}}{T_j} \right\rceil P_j + \hat{MD}_j(R_i^{mul}) + \rho_{j,i}^{mul}(R_i^{mul}) \right\} + \sum_{\forall j \in \mathrm{hp}(i)} \gamma_{i,j}^{mul} \tag{24}$$

It is important to note that, by construction, the WCRT formulation of Eq. (24) using the improved variant of the multi-set approach dominates the WCRT given by standard multi-set approach (Eq. (15)) which in turn dominates the simple union approach presented in Section V-A.

VII. Static Analysis

Having presented our proposed cache-persistence-aware WCRT analysis, we proceed by explaining how the required input quantities, defined in Section IV-B, are obtained using standard static analysis techniques integrated in WCET estimation tools.

Static cache analysis techniques use abstract interpretation to determine the worst-case behavior with respect to caches for each memory reference. The outcome of such techniques is a classification of references (e.g. *always-hit* when the reference will always result in a cache hit, *always-miss* when the reference will always result in a cache miss, *first-miss* when all successive occurrences of a reference but the first one will result in hits). The classification of each reference allows to determine if a reference will never require a memory access (*always-hit*) or may require an access to memory. For the purpose of this paper, the method presented in [18] is used.

Most WCET estimation tools use IPET (*Implicit Path Enumeration Technique*) for WCET calculation. IPET is based on an Integer Linear Programming (ILP) formulation of the WCET calculation problem [19]. This formulation reflects the program structure and the possible execution flows using a set of linear constraints. The WCET estimate for a task is obtained by maximizing the following objective function:

$$\sum_{b \in BasicBlocks} E_b \times f_b \tag{25}$$

E_b (constant in the ILP problem) is the timing information of basic block b. f_b (variables in the ILP system, to be instantiated by the ILP solver) correspond to the number of times basic block b is executed.

For a task τ_i, quantities P_i and MD_i are calculated using IPET by setting constant E_b accordingly for all basic blocks of τ_i. For the computation of P_i, only the execution time of instructions is included in E_b, ignoring memory accesses. Conversely, when computing MD_i, only memory accesses (as detected by static cache analysis) are included in E_b and the execution times of instructions are ignored.

For the particular case of direct-mapped caches, determining PCB_i and ECB_i is straight-forward. A memory block of task

τ_i belongs to PCB_i if it is the only one to map to a given cache block. ECB_i is simply the set of memory blocks of task τ_i. Determining UCB_i is achieved using the method presented in [4]. Finally, determining MD_i^r is very similar to MD_i. IPET is applied with an execution cost of 0 and considering memory accesses, but in contrast to the computation of MD_i, only memory accesses for cache blocks in $nPCB_i$ are considered.

VIII. Experiments

In this section, we evaluate the effectiveness of our proposed approaches in comparison to state-of-the-art techniques. We conducted three different experiments by varying the task utilizations, number of tasks and the size of cache and evaluated their performance in terms of schedulability.

The different inputs previously defined in Section VII were computed using the Heptane[2] static WCET estimation tool. Heptane produces upper bounds on the execution times of hard real-time applications. It computes WCETs using static analysis at the binary code level. In this paper, all experiments were conducted on C-code compiled with gcc 4.1 with no optimization for MIPS R2000/R3000. The default linker memory layout is used, i.e. functions are represented sequentially in memory, and unless explicitly stated, no alignment directive is used. Without loss of generality, all instructions are assumed to execute in *1* cycle (cache access included). Each memory access, regardless of its source, results in a penalty of $d_{mem} =$ *100* cycles. By default a direct-mapped instruction cache of size 2 KB with a line size of 32 B is considered.

We have integrated the results obtained from Heptane using static analysis with the MRTA framework developed by Altmeyer et al. [15] for multi-core response time analysis. The MRTA tool provides a compositional framework for timing verification in multi-core systems by explicitly modeling the interferences of the different components. We modified the MRTA tool to account for the new task parameters introduced in this paper. We have added a module in the MRTA framework that enables the calculation of the total CPRO $\rho_{j,i}(R_i)$ using the approaches detailed in Section V and VI. Also, as we only consider a single-core system, the preemption overhead calculation and the WCRT analysis are altered accordingly. All the experiments were performed using the Mälardalen benchmark suite [20]. Currently, we only consider the worst-case task layout where all benchmarks start at the same static memory address, thus maximizing the inter-task memory interference. The effect of different task layouts on our analysis will be explored in the future.

Evaluation is performed by randomly generating a large number of task sets and determining their schedulability using WCRT analysis for two cases:

1) WCRT analysis including only the effect of CRPD, i.e., UCB-Union multi-set (Equations (3)), and
2) Our proposed WCRT analysis that accounts for both CRPD and CPRO, i.e., CPRO Union (Equation (15)) and CPRO multi-set with/without the improvement in Equation (24).

Each task within the task set is randomly assigned parameters from the Mälardalen benchmarks. A subset of them is shown in Table I. Note that due to space limitations, it is not possible to show the details of all the benchmarks in Table I. Also it should be clear from the numbers in Table I that the benchmark suite comprises tasks with both small and big memory footprint (that fill the entire cache), consequently removing any bias in the results.

[2]https://team.inria.fr/alf/software/heptane/

TABLE I: Task parameters for a selection of benchmarks from the Mälardalen Benchmark Suite [20]

Name	C_i	P_i	MD_i	$MD^r{}_i$	ECB_i	PCB_i	UCB_i	$nPCB_i$
lcdnum	3440	984	2740	192	20	20	20	0
insertsort	7574	5974	2343	752	16	16	10	0
bs	1399	203	1223	34	11	11	9	0
bsort100	712289	710289	90893	88907	20	20	15	0
ludcmp	45135	27036	21511	18442	98	30	43	68
fdct	17350	6550	11525	9327	106	22	58	84
ud	28427	20627	10415	10415	75	53	31	22
nsichneu	316409	22009	294400	294400	1377	0	110	1377
statemate	190496	10586	180110	180110	275	0	81	275

With the exception of parameters defined in Table I, other parameters used in our experiments are defined as follows:

- The default number of tasks in each task set are 10 with task utilizations generated using UUnifast [21].
- Each task was randomly assigned one benchmark from the Mälardalen benchmark suite [20] with values of C_i, P_i, MD_i, MD_i^r along with sets of UCB, ECB, PCB and $nPCB$ obtained from the values given in Table I.
- Task periods are set according the WCET assigned to each task from the benchmarks and the randomly generated utilization, i.e., $T_i = C_i/U_i$.
- Task deadlines are implicit with priorities assigned in deadline monotonic order.

1) Total Utilization: To evaluate how our proposed WCRT analysis accounting for both CPRO and CRPD (i.e. Eq. (24) and (15)) performs in terms of schedulability in comparison to the UCB-union multi-set approach [9] (that only considers CRPD), we randomly generated 1000 task set at different utilizations varied from 0.1 to 1 in steps of 0.025. Each task set contains 10 tasks, with benchmark parameters generated for a 2 KB cache with 64 cache sets. The WCRT analysis is performed for all approaches using the same task sets. A task set is deemed unschedulable if the calculated WCRT for any task within the task set is greater than its deadline.

Figure 4a shows an average number of task sets that were schedulable using all the analyzed approaches. The graph also shows a line marked as WCRT analysis with no CRPD cost (green line) that gives an upper bound on maximum number of task set that were schedulable without considering any CRPD cost. It is also important to note that we only show a cropped version of the plot starting from a utilization of 0.6 mainly because for task set utilizations less than 0.6 all approaches produced identical results. We can see from the results that the proposed WCRT analysis accounting for both CPRO and CRPD dominates the state-of-the-art WCRT analysis (UCB-union multi-set [9]) that only accounts for CRPD. In fact, the three proposed approaches for CPRO calculation dominate the UCB-union multi-set approach [9]. This is mainly because the UCB-union multi-set approach only uses WCET (effectively the worst-case memory demand) of tasks during the WCRT analysis along with the CRPD cost defined by Equation (4),

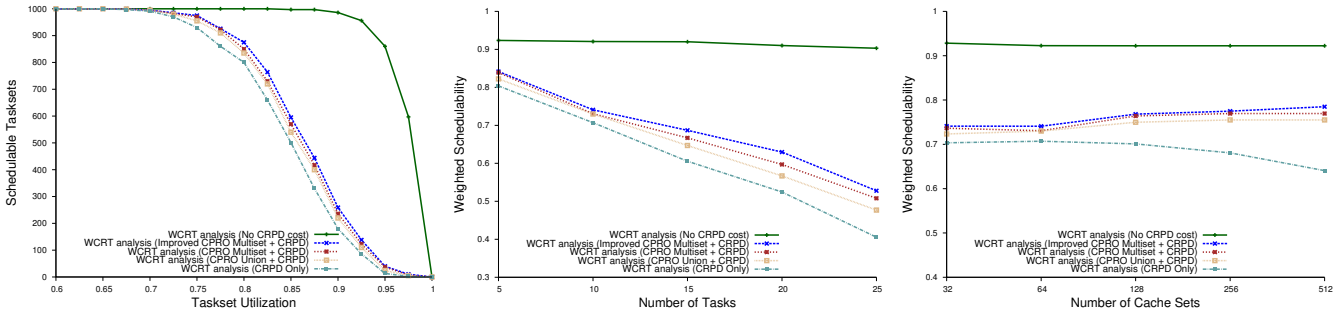

(a) Varying total utilizations (b) Varying the number of tasks (c) Varying the number of cache sets

Fig. 4: Schedulability ratio on randomly generated task sets based on the Mälardalen Benchmark

which is very pessimistic. As a result, a high number of tasks tend to be unschedulable, especially at higher utilizations.

We can also observe from the results that the CPRO multi-set approach dominates the CPRO-union and UCB-union multi-set approaches whereas, the improved CPRO multi-set approach (Eq. (24)) outperforms all the other approaches. In fact, when using the improved CPRO multi-set approach we can have substantial gains in term of schedulability in comparison to the UCB-union multi-set approach, for example at a utilization of 0.85, we gain around 10% in schedulability.

2) Number of Tasks: In preemptive systems, the number of tasks adversely affects the schedulability of the task set. To analyze the performance of all approaches w.r.t number of tasks, we varied the number of tasks from 5 to 25 increasing by 5 tasks in each step. All parameters other than the number of tasks have the same values as used in the previous section. We have used the weighted schedulability measure defined by Bastoni et al. [22] to plot the results. The weighted schedulability measure reduces what would otherwise be a 3-dimensional plot to 2 dimensions.

Figure 4b shows the results of our experiments. We can see that schedulability (varying from 0.3 to 1 by step of 0.025) for all approaches decreases as the number of tasks are increased. Indeed, this is due to an increasing number of cache evictions and reloads. On the other hand, we also observe that WCRT analysis accounting for both CPRO and CRPD performs significantly better in comparison to the other approach that only considers CRPD. The weighted schedulability using the improved CPRO multi-set approach at each point in Figure 4b is up to 10% higher than the UCB-union multi-set.

3) Cache Size: The cache size is an important factor that can affect the schedulability of tasks. If the cache is large enough to accommodate all the tasks without any cache reuse no additional memory accesses are required. In fact, in this case all the ECBs of a task will be PCBs and will never be evicted from the cache. Another case is when the cache is very small and each task can fill the entire cache during its execution. Consequently, this will result in higher memory demand for each job of the task. To evaluate the impact of cache size on the performance of the analyses, we varied the number of cache sets from 32 to 512, keeping all other task parameters constant. Figure 4c shows the resulting weighted schedulability measure for each approach as a function of the number of cache sets. As the cache line size is kept constant (i.e. 32 B), increasing the number of cache sets effectively increase the cache size. Again, we can see that our proposed WCRT analysis accounting for both CPRO and CRPD dominates the UCB-union multi-set approach [9] that only considers CRPD. In fact, by looking at the improved CPRO multi-set approach in Fig 4c, we can observe that by increasing cache size the overall schedulability also increases from 0.74 (with 32 cache sets) to 0.80 (with 512 cache sets). This is due to the fact that with a bigger cache the number of PCBs for each task will also increase (hence reducing the residual memory demand). In contrast, for the UCB-union multi-set approach (consistently with [9]), the schedulability decreases due to an increase in the number of ECBs resulting in higher preemption overheads.

IX. Conclusion

This paper builds upon the observation that a task can re-use cache contents between different jobs. A method is presented to capture these persistent cache blocks (PCBs) resulting in variable memory demand for different jobs from a task. The notion of cache-persistence reload overhead (CPRO) is introduced and different approaches are presented to calculate CPRO. These approaches are orthogonal to state-of-the-art methods used for CRPD calculation and can be used independently with any of these methods. A WCRT analysis is then presented that exploits this variable memory demand to reduce the preemption cost of higher priority tasks under fixed-priority preemptive scheduling, thereby reducing the WCRT and improving schedulability.

We evaluated the performance of our approach against a prominent approach from the state-of-the-art in terms of schedulability. Experiments were performed by varying different parameters with most of the values taken from the Mälardalen benchmarks. Experimental results show that our proposed WCRT analysis (accounting for both CPRO and CRPD) dominates the UCB-union multi-set approach (that only consider CRPD) with an average improvement of 10% in terms of schedulability.

In future work, we aim to extend this approach to multi-level set associative caches. We would like to evaluate our approach against methods such as cache coloring and cache locking. We also plan to extend our analysis to multi-core platforms.

ACKNOWLEDGMENTS

We would like to thank Sebastian Altmeyer for providing us the MRTA tool for comparison and evaluation purposes. This work was partially supported by National Funds through FCT/MEC (Portuguese Foundation for Science and Technology) and co-financed by ERDF (European Regional Development Fund) under the PT2020 Partnership, within the CISTER Research Unit (CEC/04234); by FCT/MEC and the EU ARTEMIS JU within project(s) ARTEMIS/0003/2012 - JU grant nr. 333053 (CONCERTO) and ARTEMIS/0001/2013 - JU grant nr. 621429 (EMC2); also by the European Union under the H2020 Framework Programme, within the TACLe projet (ICT COST Action IC1202, MOU: 4133/12).

REFERENCES

[1] G. C. Buttazzo, M. Bertogna, and G. Yao, "Limited preemptive scheduling for real-time systems. a survey," *Industrial Informatics, IEEE Transactions on*, vol. 9, no. 1, pp. 3–15, 2013.

[2] K. Jeffay, D. F. Stanat, and C. U. Martel, "On non-preemptive scheduling of period and sporadic tasks," in *RTSS'91*. IEEE, 1991, pp. 129–139.

[3] J. V. Busquets-Mataix, J. J. Serrano, R. Ors, P. Gil, and A. Wellings, "Adding instruction cache effect to schedulability analysis of preemptive real-time systems," in *RTAS'96*. IEEE, 1996, pp. 204–212.

[4] C.-G. Lee, J. Hahn, Y.-M. Seo, S. L. Min, R. Ha, S. Hong, C. Y. Park, M. Lee, and C. S. Kim, "Analysis of cache-related preemption delay in fixed-priority preemptive scheduling," *Computers, IEEE Transactions on*, vol. 47, no. 6, pp. 700–713, 1998.

[5] H. Tomiyama and N. D. Dutt, "Program path analysis to bound cache-related preemption delay in preemptive real-time systems," in *Proceedings of the eighth international workshop on Hardware/software codesign*. ACM, 2000, pp. 67–71.

[6] J. Staschulat, S. Schliecker, and R. Ernst, "Scheduling analysis of real-time systems with precise modeling of cache related preemption delay," in *ECRTS'05*. IEEE, 2005, pp. 41–48.

[7] Y. Tan and V. Mooney, "Timing analysis for preemptive multitasking real-time systems with caches," *ACM (TECS)*, vol. 6, no. 1, p. 7, 2007.

[8] S. Altmeyer, R. Davis, C. Maiza *et al.*, "Cache related pre-emption delay aware response time analysis for fixed priority pre-emptive systems," in *RTSS'11*. IEEE, 2011, pp. 261–271.

[9] S. Altmeyer, R. I. Davis, and C. Maiza, "Improved cache related pre-emption delay aware response time analysis for fixed priority pre-emptive systems," *Real-Time Systems*, vol. 48, no. 5, pp. 499–526, 2012.

[10] F. Nemer, H. Cassé, P. Sainrat, and A. Awada, "Improving the worst-case execution time accuracy by inter-task instruction cache analysis," in *Industrial Embedded Systems, 2007. SIES'07. International Symposium on*. IEEE, 2007, pp. 25–32.

[11] F. Nemer, H. Casse, P. Sainrat, and J. Bahsoun, "Inter-task WCET computation for a-way instruction caches," in *Industrial Embedded Systems, 2008. SIES 2008. International Symposium on*, June 2008, pp. 169–176.

[12] C. L. Liu and J. W. Layland, "Scheduling algorithms for multiprogramming in a hard-real-time environment," *JACM*, vol. 20, no. 1, pp. 46–61, 1973.

[13] R. Pellizzoni, E. Betti, S. Bak, G. Yao, J. Criswell, M. Caccamo, and R. Kegley, "A predictable execution model for COTS-based embedded systems," in *Real-Time and Embedded Technology and Applications Symposium (RTAS), 2011 17th IEEE*, April 2011, pp. 269–279.

[14] S. Altmeyer and C. M. Burguière, "Cache-related preemption delay via useful cache blocks: Survey and redefinition," *Journal of Systems Architecture*, vol. 57, no. 7, pp. 707–719, 2011.

[15] S. Altmeyer, R. I. Davis, L. Indrusiak, C. Maiza, V. Nelis, and J. Reineke, "A generic and compositional framework for multicore response time analysis," in *RTNS'15*. ACM, 2015, pp. 129–138.

[16] M. Joseph and P. Pandya, "Finding response times in a real-time system," *The Computer Journal*, vol. 29, no. 5, pp. 390–395, 1986.

[17] N. Audsley, A. Burns, M. Richardson, K. Tindell, and A. J. Wellings, "Applying new scheduling theory to static priority pre-emptive scheduling," *Software Engineering Journal*, vol. 8, no. 5, pp. 284–292, 1993.

[18] H. Theiling, C. Ferdinand, and R. Wilhelm, "Fast and precise WCET prediction by separated cache and path analyses," *Real-Time Systems*, vol. 18, no. 2-3, pp. 157–179, 2000.

[19] Y.-T. S. Li and S. Malik, "Performance analysis of embedded software using implicit path enumeration," in *LCTES '95: Proceedings of the ACM SIGPLAN 1995 workshop on Languages, compilers, & tools for real-time systems*, R. Gerber and T. Marlowe, Eds., vol. 30, no. 11, New York, NY, USA, Nov. 1995, pp. 88–98.

[20] J. Gustafsson, A. Betts, A. Ermedahl, and B. Lisper, "The Mälardalen WCET benchmarks: Past, present and future," in *OASIcs-OpenAccess Series in Informatics*, vol. 15. Schloss Dagstuhl-Leibniz-Zentrum fuer Informatik, 2010.

[21] E. Bini and G. C. Buttazzo, "Measuring the performance of schedulability tests," *Real-Time Systems*, vol. 30, no. 1-2, pp. 129–154, 2005.

[22] A. Bastoni, B. Brandenburg, and J. Anderson, "Cache-related preemption and migration delays: Empirical approximation and impact on schedulability," *Proceedings of OSPERT*, pp. 33–44, 2010.